Supplementary Information

Synergistic effect of S vacancy and P dopants in MoS_2/Mo_2C to promote electrocatalytic hydrogen evolution

Yaru Zhao [a], Wang Xin [a, b], Bitao Liu [a, b], Hongxing Li [a], Yuqing Xu [a, b], Zixuan Zhang [a]

[a] *College of Physics and Optoelectronics Technology, Baoji University of Arts and Sciences, Baoji 721016, China*

[b] *Research Institute for New Materials Technology, Chongqing University of Arts and Sciences, Chongqing, 402160, China*

Correspondence author. E-mail: liubitao007@163.com (B.T. Liu)

Contents

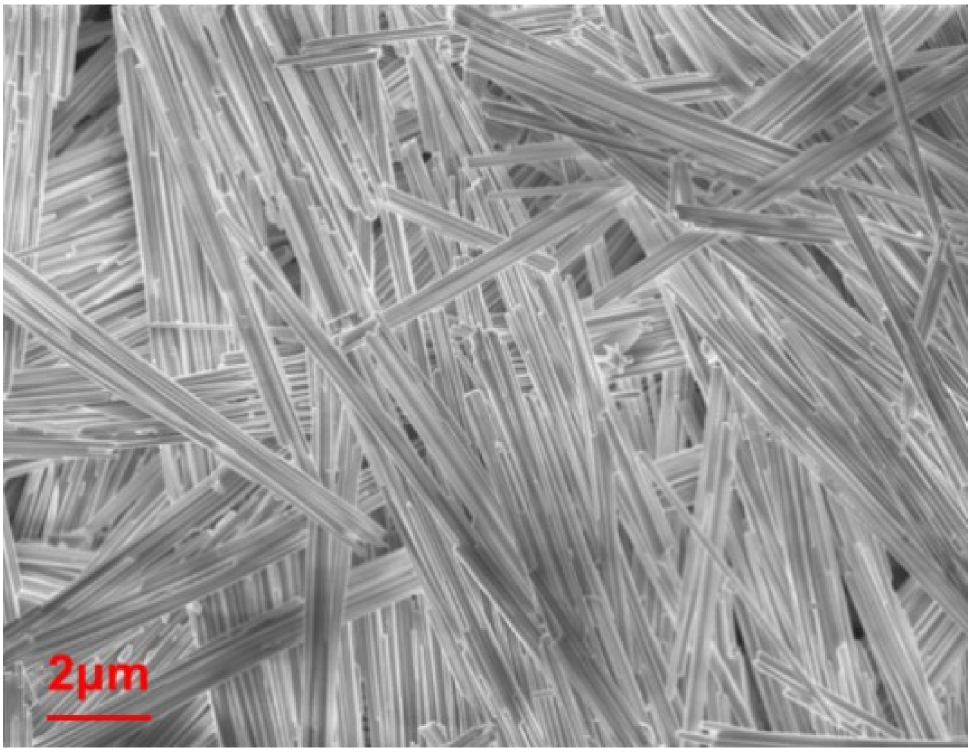

Figure S1. SEM image of Mo-MoF.

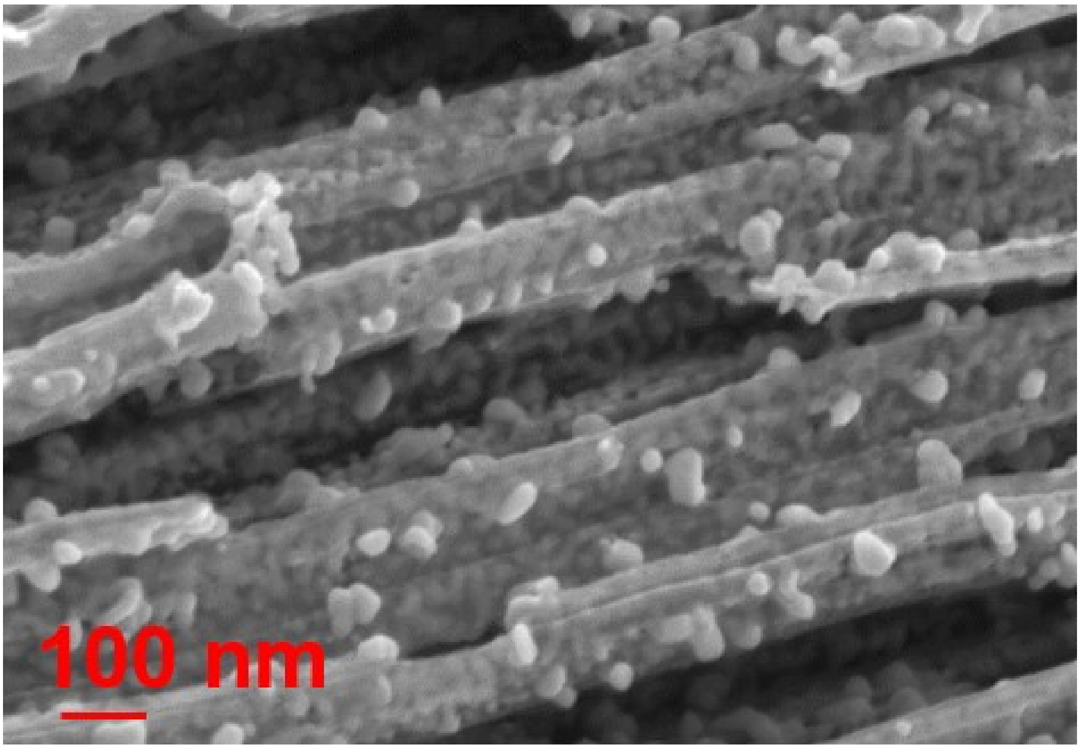

Figure S2. SEM image of Mo_2C.

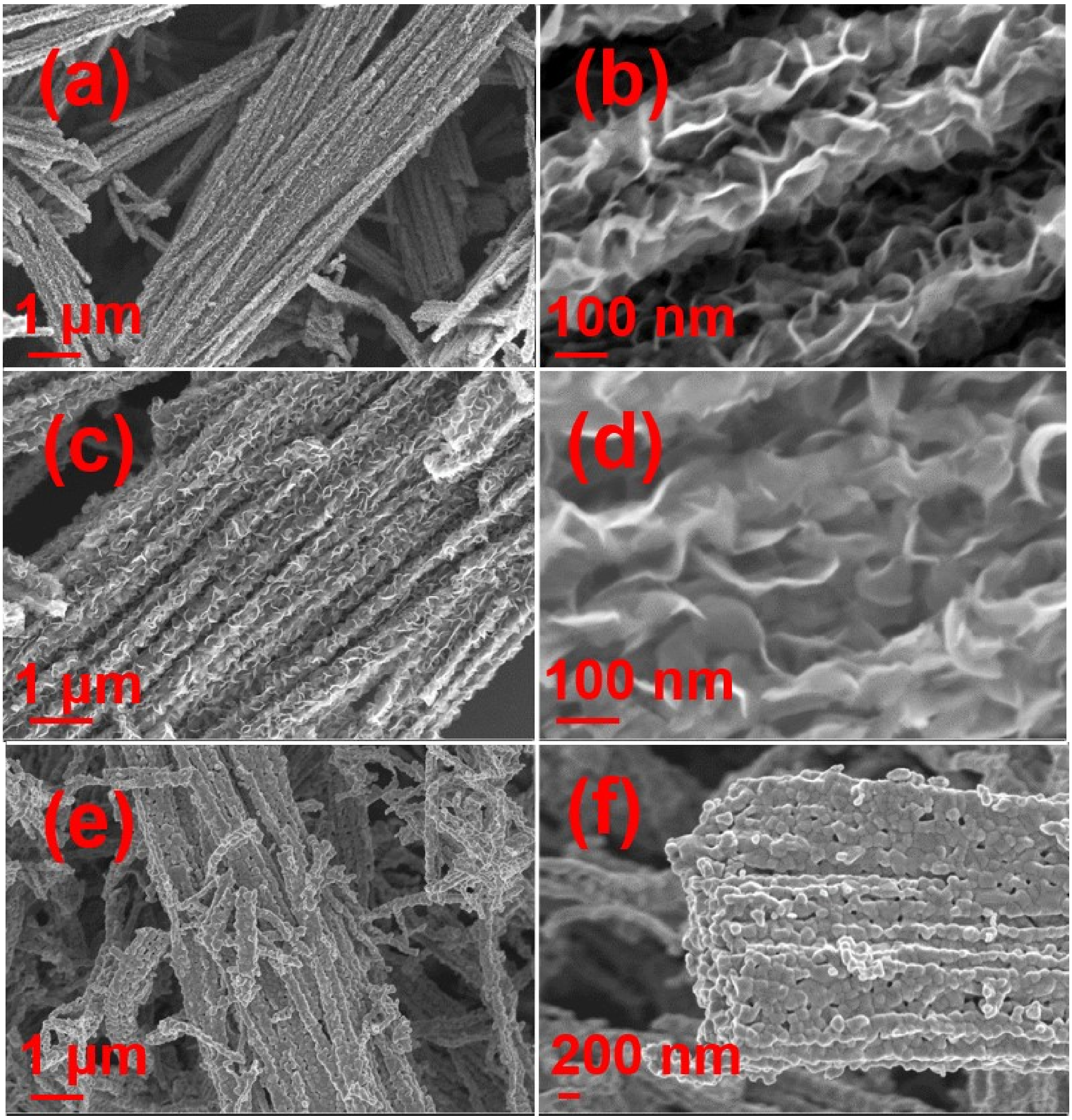

Figure S3. SEM image of different phosphating temperature (a,b) 600°C； (c,d) 700 °C; (e,f) 900 °C.

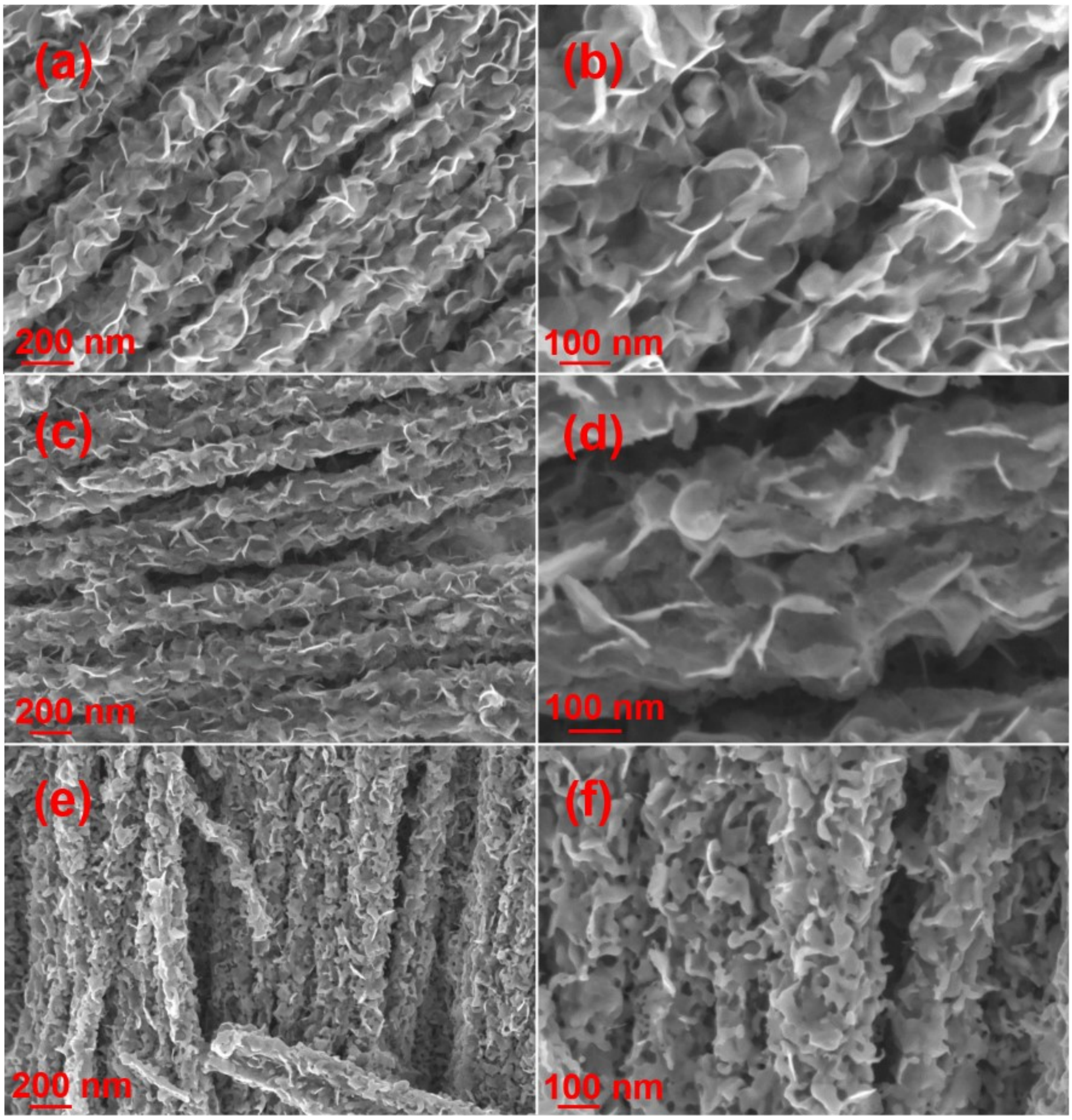

Figure S4. SEM image of different phosphorus content at 800 °C (a,b) 0.05g； (c,d) 0.2g; (e,f) 0.3g.

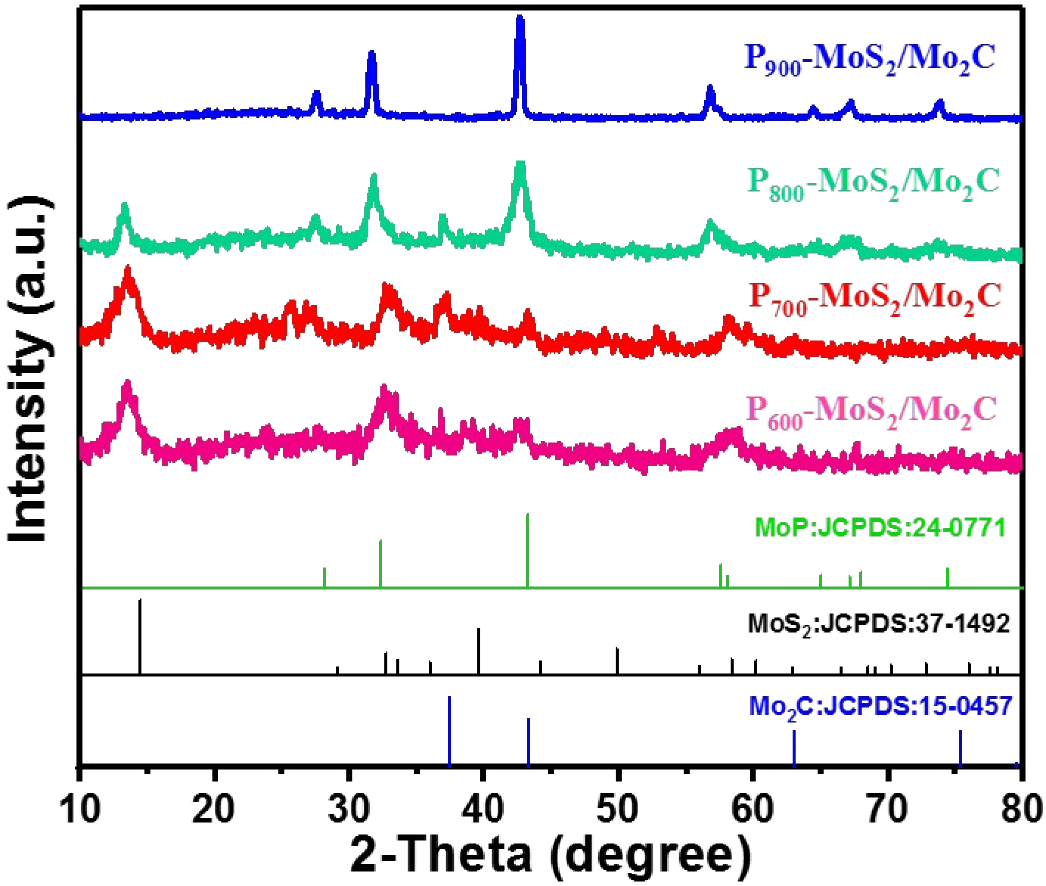

Figure S5. XRD patterns of different phosphating temperature (900°C, 800°C, 700°C, 600°C).

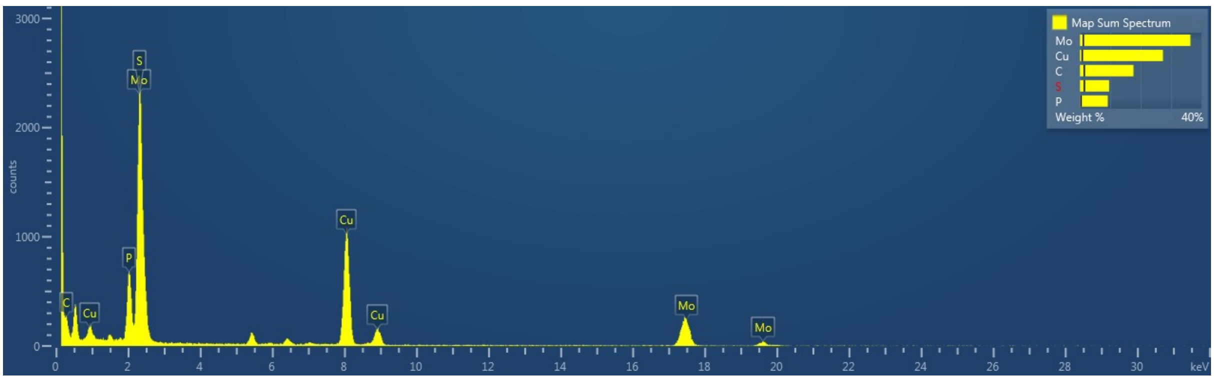

Figure S6. EDS spectra of P-MoS_2/Mo_2C.

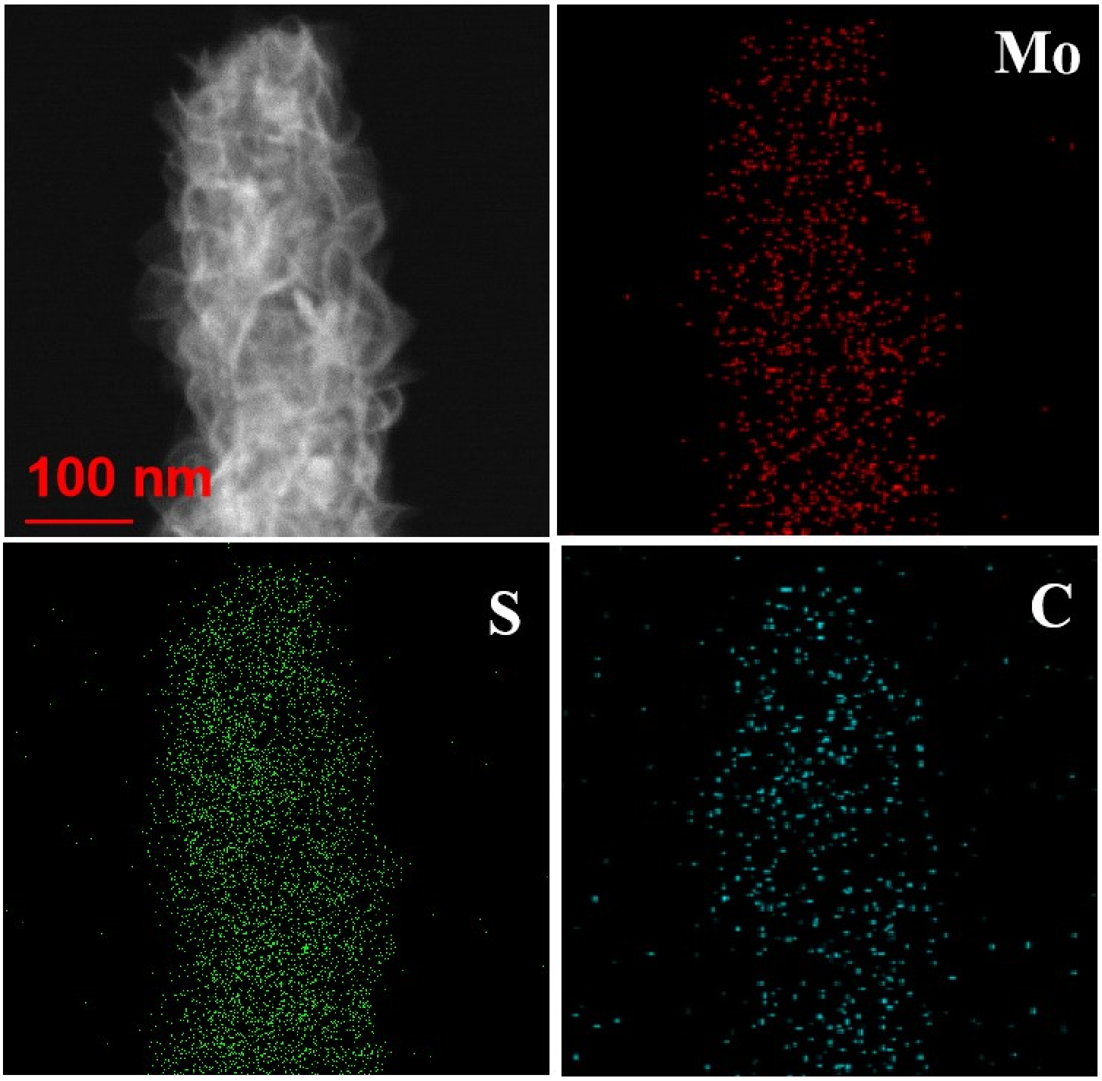

Figure S7. EDS elemental mappings of MoS_2/Mo_2C.

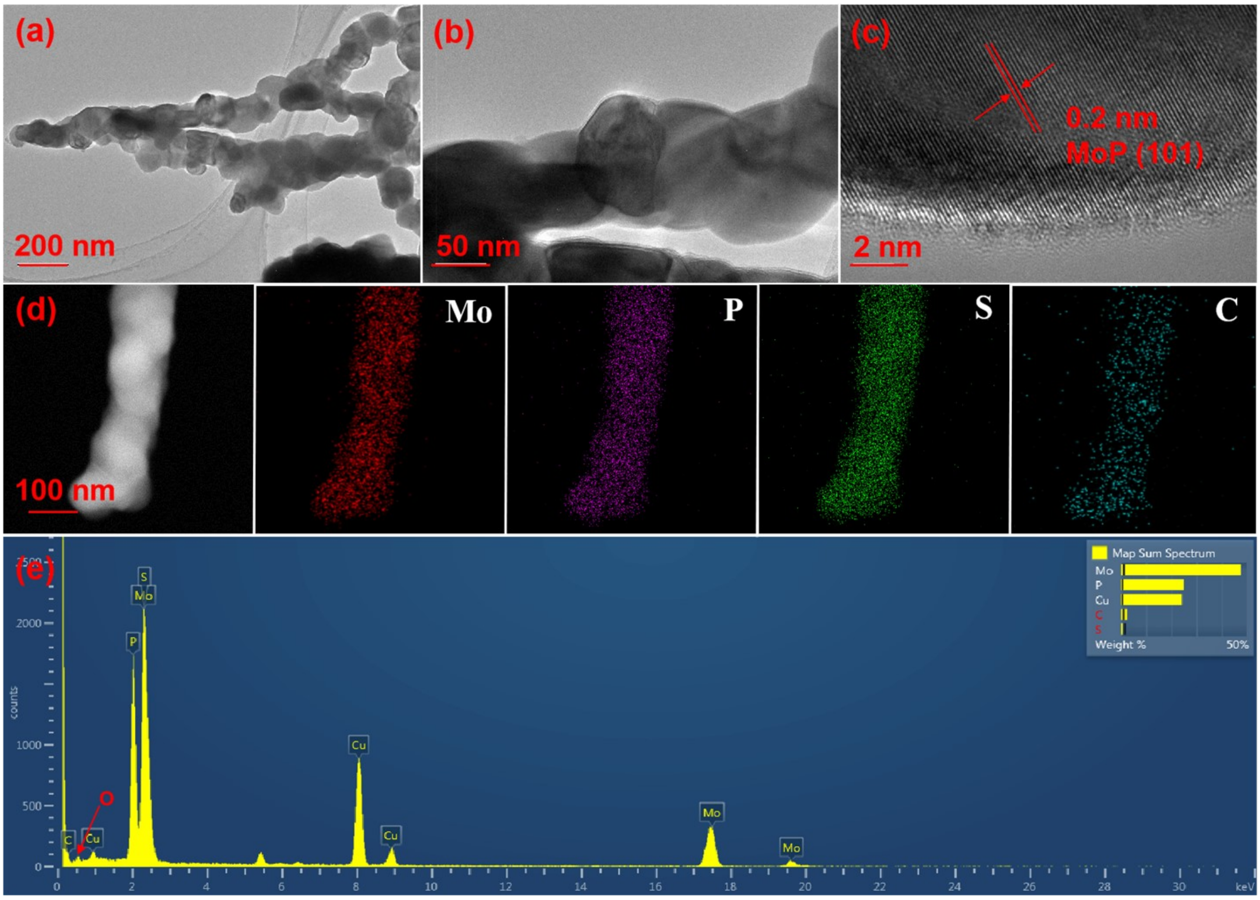

Figure S8. (a, b) TEM images and (c) HR-TEM image of P_{900}-MoS_2/Mo_2C (d) corresponding EDS elemental mappings of P_{900}-MoS_2/Mo_2C; (e) EDX spectra of P_{900}-MoS_2/Mo_2C.

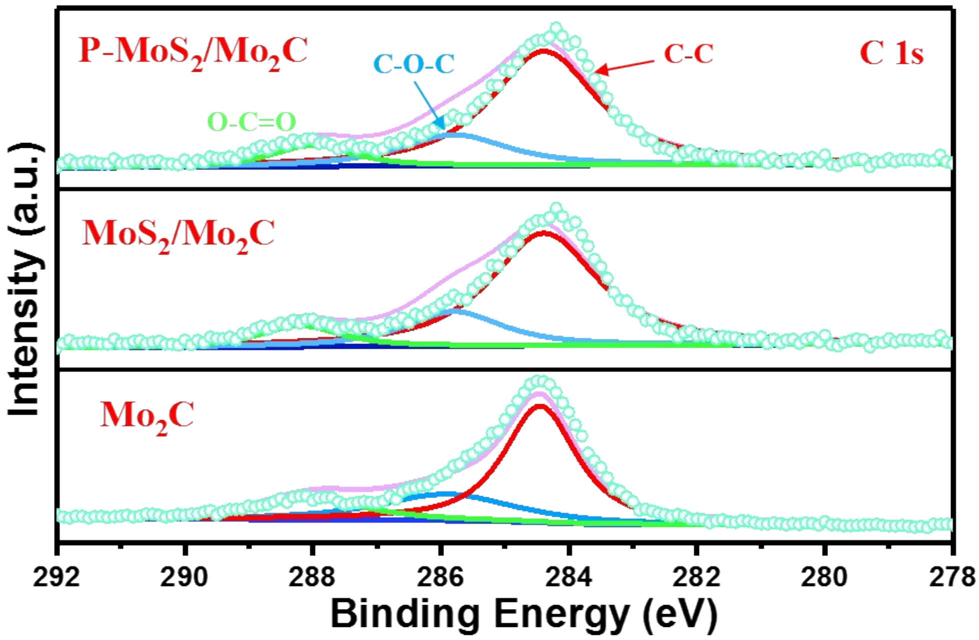

Figure S9. C 1s XPS of P-MoS_2/Mo_2C, MoS_2/Mo_2C and Mo_2C.

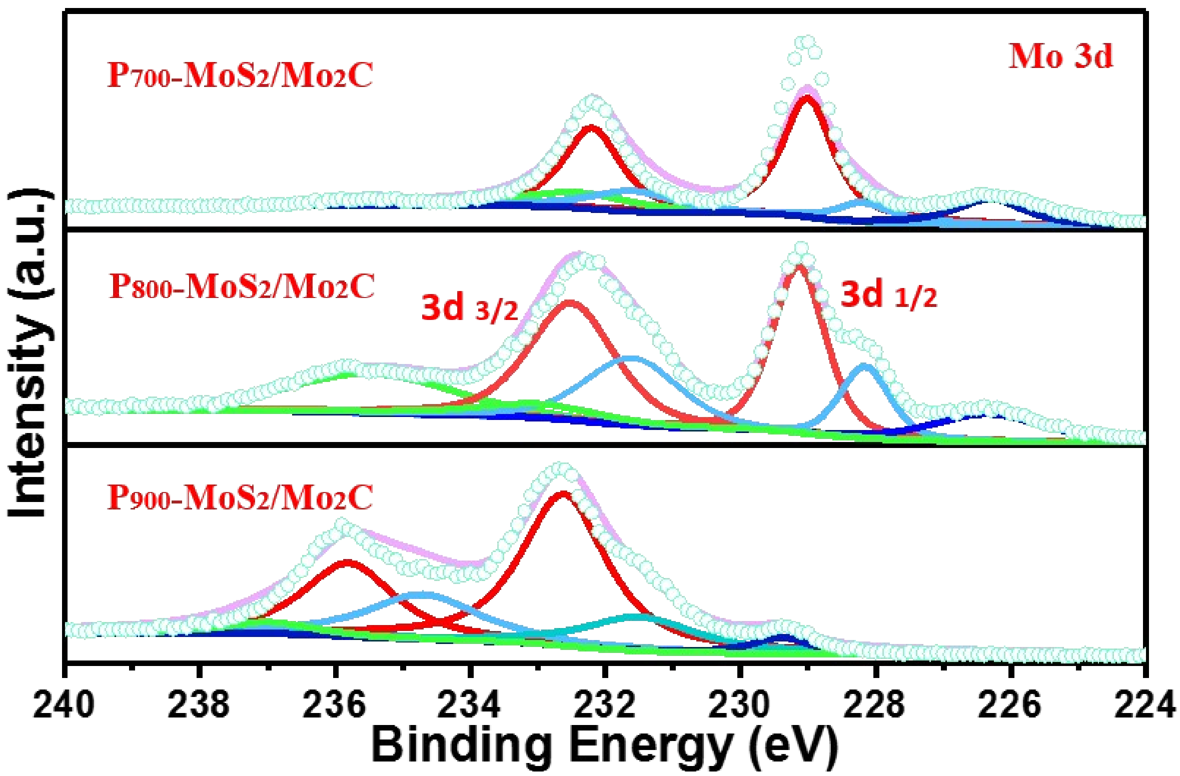

Figure S10. XPS of Mo 3d in different phosphating temperature (700°C, 800°C, 900°C).

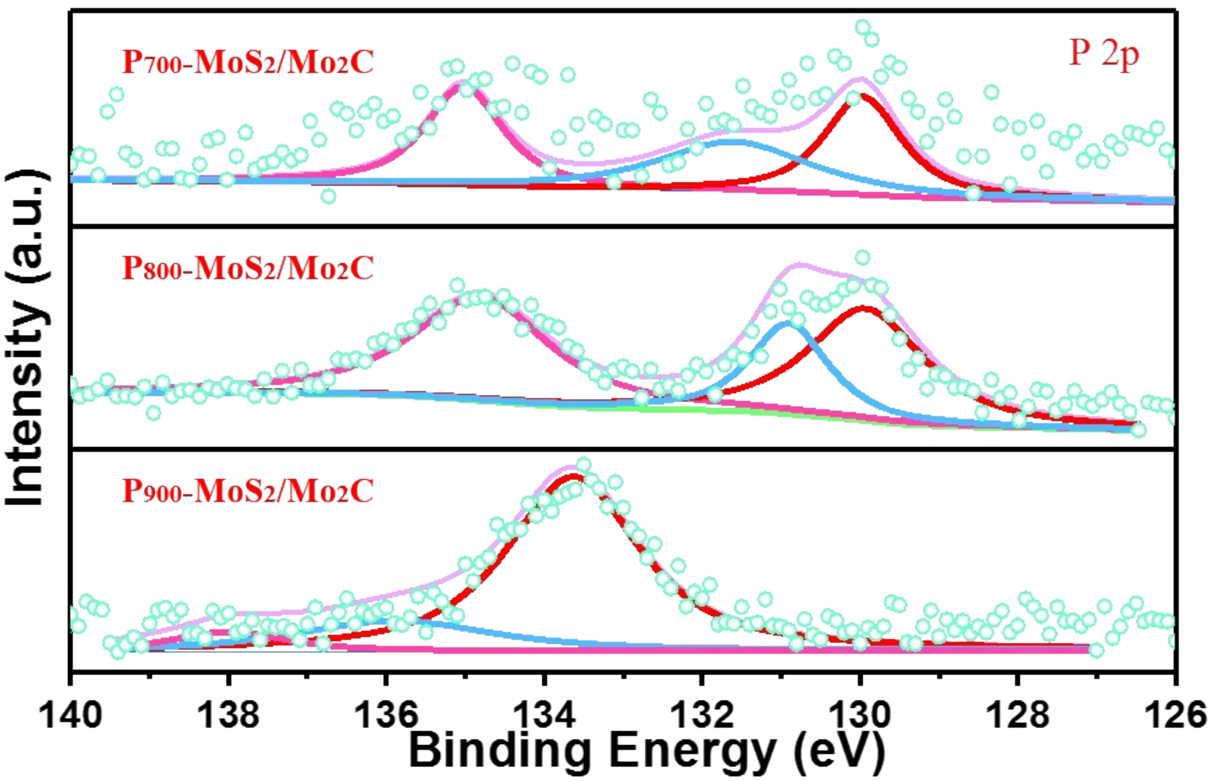

Figure S11. XPS of P 2p in different phosphating temperature (700°C, 800°C, 900°C)

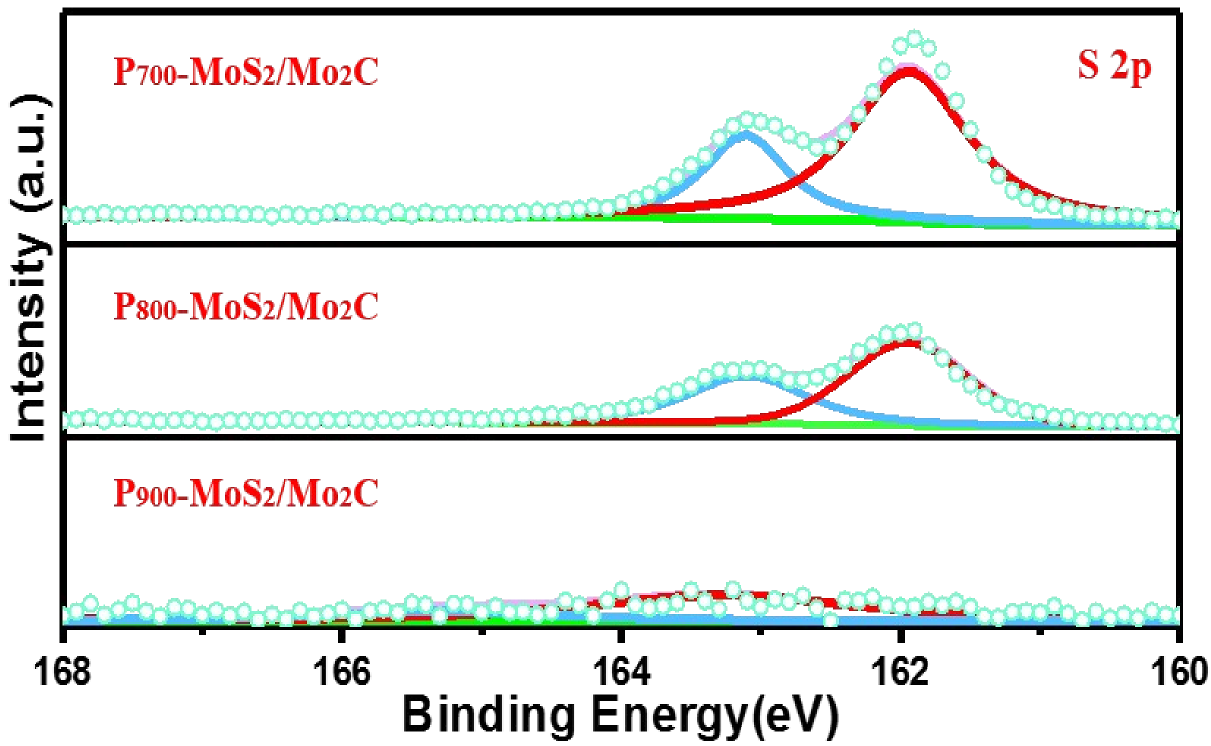

Figure S12. XPS of S 2p in different phosphating temperature (700°C, 800°C, 900°C)

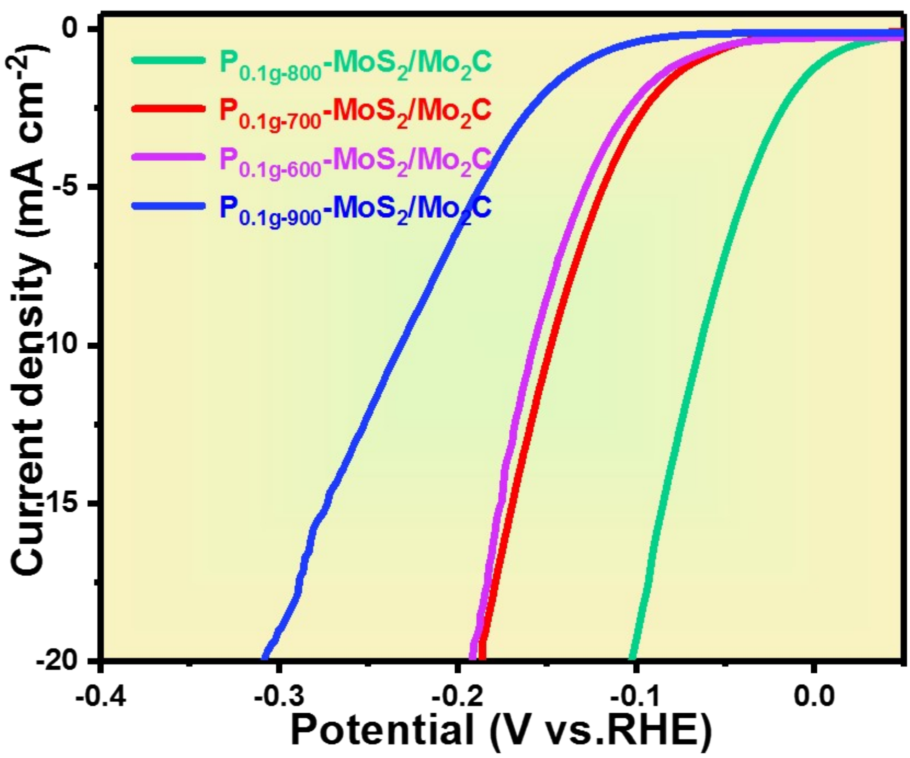

Figure S13. HER polarization curves tested at different phosphating temperature (900°C, 800°C, 700°C, and 600 °C) in 1 M KOH.

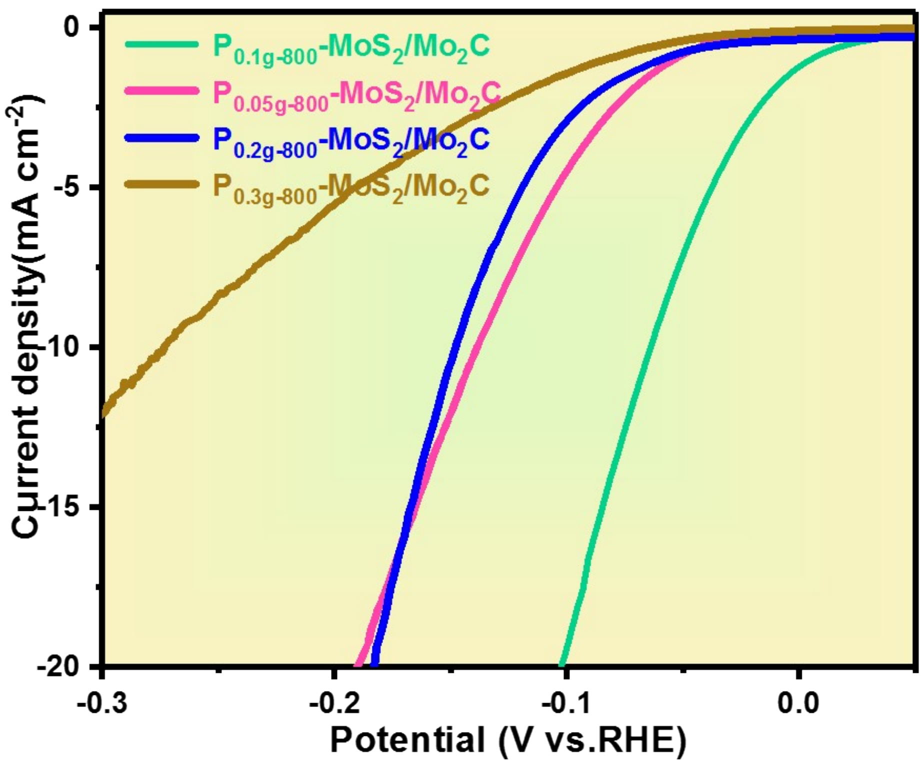

Figure S14. HER polarization curves tested of different phosphorus content (0.05, 0.1, 0.2, and 0.3 g) at 800°C.

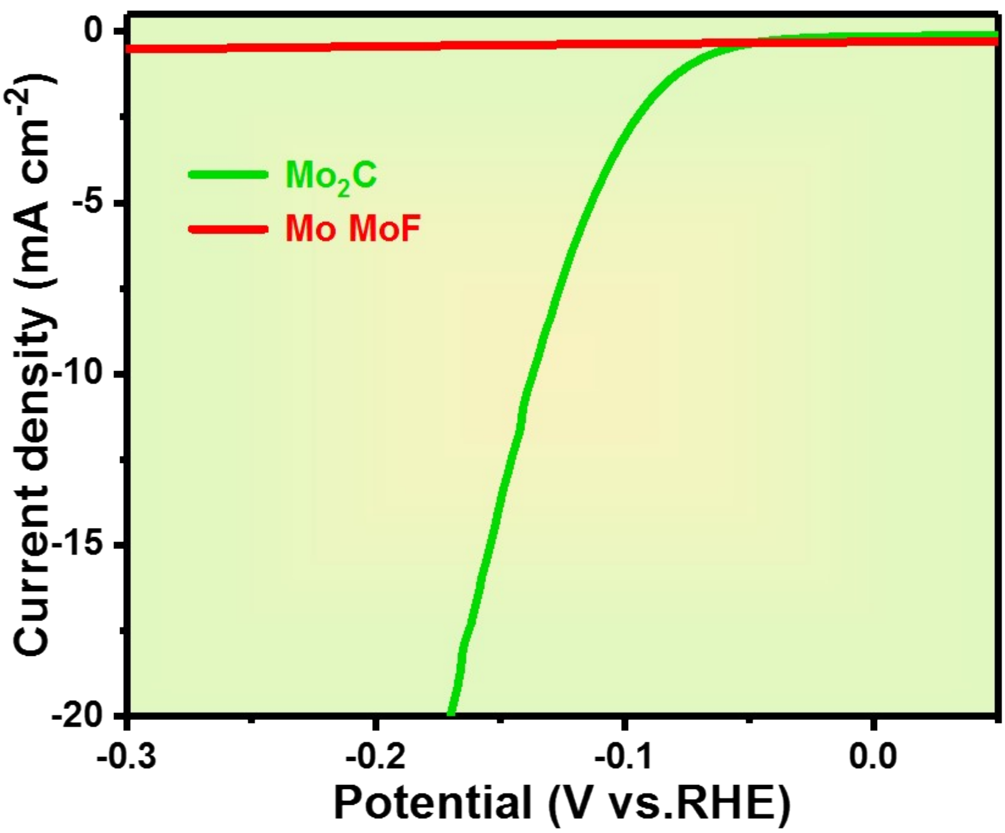

Figure S15. HER polarization curves tested of Mo_2C and Mo MOF.

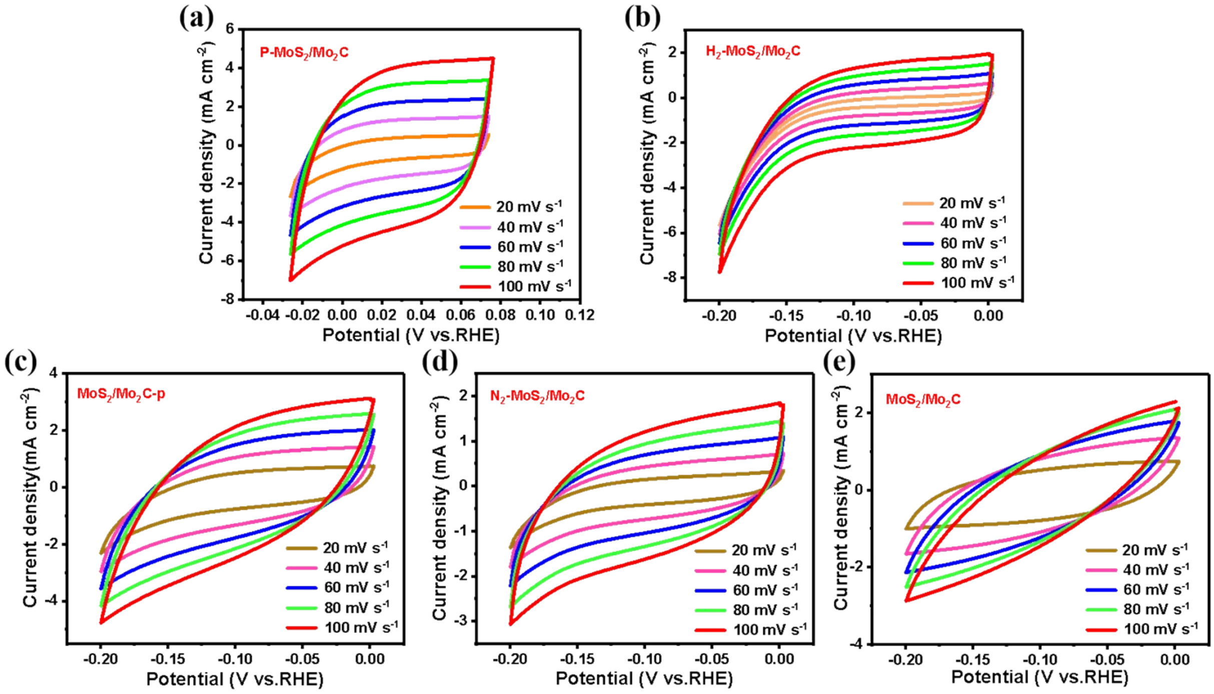

Figure S16. Typical cyclic voltammograms at different scan rates from 20 to 100 mV s^{-1}. (a) P-MoS_2/Mo_2C; (b) H_2-MoS_2/Mo_2C; (c) MoS_2/Mo_2C-p; (d) N_2-MoS_2/Mo_2C and (e) MoS_2/Mo_2C. The scanning potential range is from 1.023 V to 1.223V vs SCE.

Table S1. Summary of various MoS_2-based catalysts for HER in 1 M KOH.

Catalyst	**η_{10} (mV)**	**Tafel slope (mV dec^{-1})**	**Reference**
P-MoS_2/Mo_2C	66	67	This work
H-MoS_2/MoP	92	59	Small, 2020, 16, 2002482 [1]
N-MoP/CC	70	_	Appl. Catal. B: Environ., (2019) 118441 [2]
MoS2/Mo2C	63	48	ACS Catal.,(2017),7,7312-7318[3]
MoS_2/$CoNi_2S_4$	78	67.4	Adv. Funct. Mater.,(2019) 1908520 [4]
MoS_2 /NiCoS	189	75	J. Mater. Chem. A, 2019, 7, 27594-27602 [5]
NiS/MoS_2	174	70.2	J. Mater. Chem. A, 2019,7,21514-21522 [6]
MoS_2	153	73	ACS Energy Lett. 2019, 4, 2830-2835 [7]
CuS@MoS_2	135	50	J. Colloid Interface Sci., 2020, 564, 77-87 [8]
N-doped MoS_2	114	46.8	J. Am. Chem. Soc. 2019, 141, 18578-1858 [9]
CoP/CN@MoS_2	149	88	ACS Appl. Mater. Interfaces 2019,11, 366 [10]

References

1. Q. Liu, Z. Xue, B. Jia, Q. Liu, K. Liu, Y. Lin, M. Liu, Y. Li and G. Li, Hierarchical nanorods of MoS_2/MoP heterojunction for efficient electrocatalytic hydrogen evolution reaction, *Small*, 2020, **16**, 2002482.
2. C. G. López-Calixto, M. Liras, V. A. de la Peña O'Shea and R. Pérez-Ruiz, Synchronized biphotonic process triggering CC coupling catalytic reactions, Applied Catalysis B: Environmental, 2018, **237**, 18-23.
3. Z. Zhao, F. Qin, S. Kasiraju, L. Xie, M.Alam, Vertically Aligned MoS_2/Mo_2C hybrid Nanosheets Grown on Carbon Paper for Efficient Electrocatalytic Hydrogen Evolution, ACS Catal., 2017, **7**, 7312-7318.
4. J. Hu, C. Zhang, P. Yang, J. Xiao, T. Deng, Z. Liu, B. Huang, M. K. H. Leung and S. Yang, Kinetic-Oriented Construction of MoS 2 Synergistic Interface to Boost pH-Universal Hydrogen Evolution, Adv. Funct. Mater., 2019, **30**, 1908520.
5. C. Qin, A. Fan, X. Zhang, S. Wang, X. Yuan and X. Dai, Interface engineering: few-layer MoS_2 coupled to a NiCo-sulfide nanosheet heterostructure as a bifunctional electrocatalyst for overall water splitting, Journal of Materials Chemistry A, 2019, **7**, 27594-27602.
6. A. Long, W. Li, M. Zhou, W. Gao, B. Liu, J. Wei, X. Zhang, H. Liu, Y. Liu and X. Zeng, MoS_2 nanosheets grown on nickel chalcogenides: controllable synthesis and electrocatalytic origins for the hydrogen evolution reaction in alkaline solution, Journal of Materials Chemistry A, 2019, **7**, 21514-21522.
7. H. A. Ariyanta, T. A. Ivandini and Y. Yulizar, A novel way of the synthesis of three-dimensional (3D) MoS_2 cauliflowers using allicin, Chem. Phys. Lett., 2021, **767**, 138345.
8. L. Liu, X. Liu and S. Jiao, CuS@defect-rich MoS_2 core-shell structure for enhanced hydrogen evolution, J. Colloid Interface Sci., 2020, **564**, 77-87.
9. H. Wang, X. Xiao, S. Liu, C.-L. Chiang, X. Kuai, C.-K. Peng, Y.-C. Lin, X. Meng, J. Zhao, J. Choi, Y.-G. Lin, J.-M. Lee and L. Gao, Structural and Electronic Optimization of MoS_2 Edges for Hydrogen Evolution, J. Am. Chem. Soc., 2019, **141**, 18578-18584.
10. J.-G. Li, K. Xie, H. Sun, Z. Li, X. Ao, Z. Chen, K. K. Ostrikov, C. Wang and W. Zhang, Template-Directed Bifunctional Dodecahedral CoP/CN@MoS_2 Electrocatalyst for High Efficient Water Splitting, ACS Appl. Mater. Interfaces, 2019, **11**, 36649-36657.